# Multiple source modulated molecular beam reactive scattering applied to hydrogen recombination and oxidation on the Rh(111) surface

D. F. Padowitz[a] and S. J. Sibener
*The James Franck Institute and The Department of Chemistry, The University of Chicago, Chicago, Illinois 60637*

(Received 20 November 1990; accepted 15 March 1991)

Surface kinetics which are nonlinear and involve multiple reactants are not amenable to standard modulated molecular beam reactive scattering techniques. To explore these complex reactions, we have developed a new three molecular beam arrangement. Two continuous, independently adjustable beams establish steady state surface concentrations, while a third weaker beam is modulated to induce small concentration perturbations around the selected steady state. This permits experimental linearization of nonlinear kinetics over a wide range of coverages, helping us to evaluate coverage dependent rate constants and to isolate individual elementary steps from complex reaction mechanisms. The technique has been applied to the oxidation of hydrogen to water on the Rh(111) surface. We have demonstrated linearization of the water reaction with isotopic substitution forming HDO. The analysis is illustrated by the simpler example of hydrogen–deuterium recombination. HD shows an activation energy of 20 kcal/mol and preexponential on the order of $10^{-2}$ cm$^2$ s$^{-1}$ for the linearized reaction in the low coverage limit.

## I. INTRODUCTION

### A. MBRS and nonlinear kinetics

Molecular beam scattering techniques have become major tools for studying the kinetics and dynamics of gas–surface interactions. Molecular beams have many advantages for surface reaction kinetics. They provide a high reactant flux at the surface with low background pressures. Since there are no gas phase collisions, only surface reactions are observed, and rates are not limited by gas phase diffusion to or from the surface. Sensitivity is further increased when the molecular beam is modulated so that background signals can be rejected. Modulated molecular beam relaxation spectrometry (MBRS), a descendant of Eigen's pioneering work on chemical relaxation,[1] gives us kinetic information in the dynamic response of surface processes to a time dependent beam flux. In a simple case, a chopped beam of a single species is scattered from a surface and detected. The phase lag of the detected beam depends on the surface residence time, which yields adsorption and desorption kinetics. Relaxation techniques with reactive scattering, in which new chemical species are formed, are widely used to study heterogeneous chemical reactions. Here beams of two or more reactants are scattered from the surface and the product flux is measured. Kinetic information is contained in the time dependent response of the product flux to modulation of one of the reactants.

Extracting rates from MBRS data is straightforward if the response to changing reactant flux is linear.[2] Accordingly, most studies reported to date have been on simple linear reactions, such as single component adsorption–desorption at low coverage, or have used linear approximations for weakly nonlinear systems, or have worked in a pseudo-first order regime over a limited coverage range.[3–8]

In general, chemical reactions are not linear. An elementary bimolecular step in a reaction involves two species and the rate of reaction depends on the product of their concentrations. If both concentrations change with time, the mechanism will not be linear. A reaction will also be nonlinear if the rate constants change with concentration. This is frequently true for surface reactions, because adsorption probabilities, preexponential factors, and activation energies often depend on coverages.

For nonlinear reactions it becomes difficult not only to extract rates from experimental data, but also to analyze postulated mechanisms for comparison to those rates. Usually, linear transform methods such as Fourier transform deconvolution are used to separate kinetics from instrumental factors. These methods cannot be applied to nonlinear systems. Furthermore, nonlinear model mechanisms may defy mathematical analysis. Foxon *et al.* and other early workers were well aware of these constraints, and anticipated the necessity for linearized MBRS.[3] In the succeeding years however, the numerous successes of MBRS obscured these limitations, which have only recently been reconsidered as more complex reactions are encountered.

### B. Linearized MBRS with multiple beams

Fortunately, during an experiment it is often possible to restrict the reaction to a linear regime. In the most limited case, the response may be linear if the intensity of the modulated beam is kept very low. This is not generally satisfactory, since the reaction can then be observed only at low coverages. A more general approach has been known in principle for many years: a small modulation superimposed on a larger continuous reactant flux. For a sufficiently small perturbation, relaxation to the steady state is linear. Then linear transform analysis may be applied to the experimental data, and the differential equations for a postulated mecha-

 0734-2101/91/042289-13$01.00  

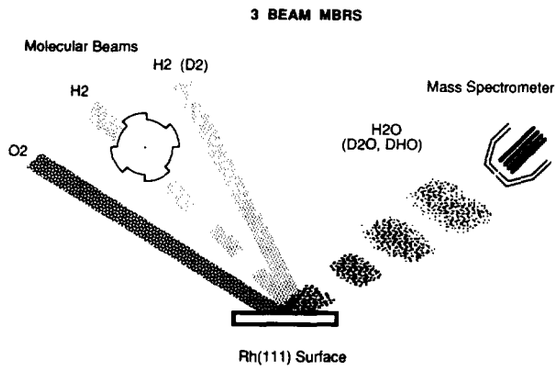


FIG. 1. Multiple source MBRS. Two continuous, independently adjustable beams establish steady state conditions, the third modulated beam perturbs the steady state. In addition to linearization by weak perturbation, this configuration permits great experimental flexibility, as in the isotopic substitution shown here.

nism may be solved by series expansions or perturbation techniques, so that we can obtain the kinetic information we seek. If this linearization can be performed for different steady state conditions, the reaction mechanism or coverage dependence of the rate constants may be determined over the global range of a nonlinear reaction.

To implement this approach for complex reactions, we have introduced a new *three* molecular beam scattering arrangement. The scheme is depicted in Fig. 1. We use two continuous, independently adjustable beams to establish a steady state on the surface, while a weaker modulated third beam induces small concentration perturbations around the selected steady state.

Since linearization requires a weak modulated beam, linearized MBRS is often forced to work near the zero coverage limit. Using an additional continuous beam of the modulated reactant allows us a wider range of surface coverages. This is important to determine coverage dependent activation energies and preexponential factors. By controlling reactant and intermediate coverages, sometimes using isotopic substitutions in the beams, we can explore regimes in which different pathways may dominate the mechanism. Most significantly, we may be able to isolate the individual elementary steps which compose complex reaction mechanisms.

This paper will concentrate on the technique, using hydrogen recombination and oxidation on Rh(111) as examples. The most fundamental surface reaction, the recombination of hydrogen, already exhibits nonlinearity. While this reaction only requires two molecular beams, it is the simplest example of the essential principles of experimental linearization and perturbation analysis of the mechanism. A more complex reaction, the oxidation of hydrogen to water, will illustrate the general utility of multiple beams. A separate publication contains more extensive results on water formation on Rh(111).[9]

## II. EXPERIMENT

The surface scattering machine consists of a removable source chamber containing three supersonic molecular beam sources and a main chamber with sample and manipulator, mass spectrometer detector, residual gas analyzer, Auger spectrometer and sputter ion gun. Descriptions of the machine are found in Refs. 10 and 11. Here we will emphasize molecular beam source configuration and data collection.

The source chamber was divided laterally into two sections, each with three regions of differential pumping before the main chamber. The left beam was in one section and the center and right beams together in the other. The mechanical pump backing the left side contained oxidation resistant oil. The sources consisted of $\approx 100\,\mu$ apertures or pinholes, each with a skimmer, collimator, and shutter. The center beam was modulated by a chopper wheel with a four slot 50% total duty cycle pattern, or by a dual pattern chopper with two 25% slots and two 1% slits for time-of-flight measurements. The wheel was spun at at 10–400 Hz.

The hydrogen beams had a mean velocity $v_0 = 2.4$–$2.7\times10^5$ cm/s and spread $\alpha = 8.8\times10^3$–$1.6\times10^4$ cm/s. Maximum side beam fluxes were on the order of 10 L/s, or $10^{-5}$ Torr cm$^{-2}$. The base pressure in the scattering region was $5\times10^{-11}$ Torr, rising to $6\times10^{-9}$ Torr at the highest beam fluxes.

In these experiments the sample was a rhodium single crystal cut and polished within 1/2° of the face-centered-cubic (fcc) (111) plane using standard techniques. The distance from chopper to sample was 21.21 cm. On the sample, the center beam spot was contained within the overlap of the left and right beam spots. On entering the main chamber the left and right beams were defined by 80 mil apertures, and the center beam by a 40 mil aperture. The side beams were 15° off axis, and the sample normal was usually inclined 45° to the beam axis. This resulted in roughly $5\times7$ mm elliptical spots on the sample, which overlap the center $2.5\times3.25$ mm modulated beam spot.

The detector was a differentially pumped quadrupole mass spectrometer. Acceptance angle of the detector was 1°. Flight path from sample to ionizer was 14.45 cm. At normal, the detector viewed a spot of $\approx 2.5$ mm diam.

Arrival times of products at the mass spectrometer were recorded by a custom multichannel scalar system interfaced to a CAMAC system and an LSI-11/23 compatible computer. The scalar had negligible dead time between channels and a minimum dwell time of 0.25 $\mu$s. Typically 255 channels of 5–20 $\mu$s were collected. Data acquisition was triggered by a photodetector on the chopper wheel assembly. For the present experiments, good quality time-of-arrival wave forms usually required 10–60 min of signal averaging. A typical run of 20 min at 400 Hz chopper speed would be $5\times10^5$ chopper periods or "shots" giving $5\times10^4$ counts/channel with signal to background of 2, and S/N of 200.

## III. RESULTS AND DISCUSSION

### A. Overview

We begin by pointing out the origins of nonlinear kinetics in possible mechanisms for hydrogen recombination and water formation. In a brief review of linear MBRS methods and analysis, we show typical results for the production of water

and describe "transfer function" analysis of linear systems. We next discuss the problems for both experiment and analysis caused by nonlinear reactions. Nonlinearities are shown to emerge in the water reaction at low temperatures. We then introduce the multiple beam approach. This method is first used to control surface coverage in the water reaction, to reduce problems at low temperature, and to examine coverage dependent kinetics. Next we look at isotopic substitution in water, which graphically reveals nonlinearity. Turning to the simpler HD recombination reaction, we analyze the origin of the nonlinearity, linearize the reaction, and perform a perturbation analysis of the mechanism. Finally returning to water, we demonstrate the linearization of the reaction, although we do not do a complete analysis.

## B. Prototype systems

### 1. HD recombination

Nonlinearities are already present in the most fundamental surface reaction. In recombination of hydrogen and deuterium nonlinearity arises from bimolecular recombination steps and from coverage dependent sticking and desorption.

$$H_{2gas} \overset{s_0[1-(H+D)]}{\underset{k_{dH_2}}{\rightleftarrows}} 2H, \tag{1}$$

$$D_{2gas} \overset{s_0[1-(H+D)]}{\underset{k_{dD_2}}{\rightleftarrows}} 2D, \tag{2}$$

$$H + D \overset{k_1}{\underset{k_{-1}}{\rightleftarrows}} HD, \tag{3}$$

$$HD \overset{k_dHD}{\rightarrow} HD_{gas}. \tag{4}$$

The recombination step is nonlinear if both [H] and [D] vary, and the rate constants $k_d$ are coverage dependent. The literature on the $H_2 + D_2 \rightarrow 2HD$ recombination reaction is extensive. The reader is referred to review articles such as Ref. 12.

### 2. Hydrogen oxidation on Rh(111)

While hydrogen recombination will introduce the principles of linearization, a more complex reaction will illustrate the general utility of multiple beams. The oxidation of hydrogen to form water on the Rh(111) surface is not yet completely understood despite considerable effort.[13] Consider the plausible, though simplified mechanism:

$$H_{2gas} \overset{s_0[1-([H]+[O])]^2}{\underset{k_{dH_2}}{\rightleftarrows}} 2H, \tag{5}$$

$$O_{2gas} \overset{s_0(1-[O])^2}{\underset{k_{dO_2}}{\rightleftarrows}} 2O, \tag{6}$$

$$O \overset{k_{bulk}}{\underset{k_{surf}}{\rightleftarrows}} O_{bulk}, \tag{7}$$

$$H + O \overset{k_1}{\underset{k_{-1}}{\rightleftarrows}} OH, \tag{8}$$

$$H + OH \overset{k_2}{\underset{k_{-2}}{\rightleftarrows}} H_2O, \tag{9}$$

$$2OH \overset{k_3}{\underset{k_{-3}}{\rightleftarrows}} H_2O + O, \tag{10}$$

$$H_2O \overset{k_{dH_2O}}{\rightarrow} H_2O_{gas}. \tag{11}$$

Hydrogen and oxygen are dissociatively chemisorbed on Rh(111) above room temperature. Hydrogen sticking probabilities and desorption rate parameters depend on both hydrogen coverage and oxygen coadsorption.[14,15] The terms $s_0$ are the sticking fractions at zero coverage. Coverage dependent adsorption is represented in the $(1 - [O])$ terms, which may be first order at low temperatures if there are molecular precursors, otherwise they are second order. Oxygen has very complex behavior on the rhodium surface, including dissolution into the bulk metal and possibly island formation.[14] Bulk solution of oxygen is Eq. (7). At high temperatures water formation most likely proceeds through sequential addition of hydrogen to oxygen with a hydroxyl intermediate. Hydroxyl disproportionation, Eq. (10), may become important at low temperatures and high coverages. The final step is the desorption of water. Each of the coverage dependent rate constants and the terms which are quadratic in hydrogen concentration introduce nonlinearities which may appear in the observed reaction.

## C. MBRS for linear systems

As described in Sec. II, a typical MBRS apparatus consists of a source for molecular beams of reactants, a catalytic or reactive sample surface, and a mass spectrometer to detect products leaving the surface. One of the reactant beams is modulated with a spinning chopper wheel or perhaps a shutter. Early work used lock-in detection to measure the phase and amplitude of the product at the chopper frequency. Most current experiments use fast electronics to record the full time dependence of the product flux following a reactant pulse. The detector signal is multichannel averaged over many modulation periods to obtain the product "time-of-arrival wave form."

Waveforms for water produced on the Rh(111) surface

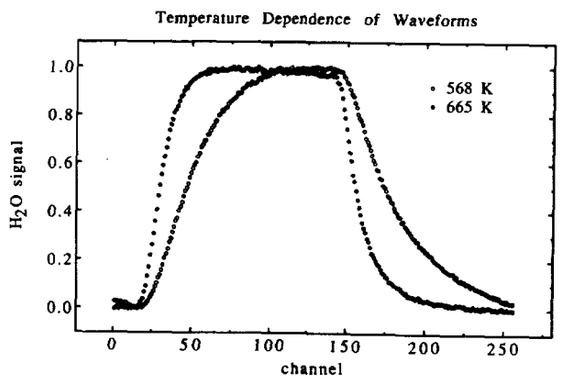


FIG. 2. Kinetic information is obtained from the temperature dependence of the waveforms. The phase lag, seen in the slower rise and fall at lower temperature, indicates a longer "surface residence time" or lower reaction rate.

by reaction of a modulated hydrogen beam and a continuous oxygen beam are shown in Fig. 2. The surface temperatures were 665 and 568 K. The hydrogen modulation was nearly a square wave. Water formed on the surface shows a more gradual rise and fall, slower at low temperature. As a first approximation we might try an exponential fit to the rising and falling edges. This is equivalent to assuming a single step first order reaction. The time constant for a single exponential lag $\tau$ is the inverse of the first order rate constant: $k = 1/\tau$ and so $\ln(\tau) = -\ln(k)$. For water formation from 500–800 K, $1/\tau$ exhibits approximately Arrhenius behavior. Assuming a single step, we obtain $E_a = 6.8 \pm 0.4$ kcal/mol, and $A = 10^6$–$10^7\ s^{-1}$. However, more sophisticated analysis of the wave forms will indicate that this is incorrect, and that a serial mechanism of two or more steps is required.

### 1. Transfer function analysis of linear surface kinetics

The "transfer function" is the response of a system to a delta function input or impulse. In kinetics, this might be relaxation to a steady state following a transient concentration jump. It is often convenient to examine the transfer function in the frequency domain. Since an impulse contains all frequencies, the transfer function is the phase and amplitude of the product signal for all input frequencies. From the variation of the transfer function with reactant flux, surface temperature, or other parameters, an outline of the dominant steps of the mechanism may be deduced. For simple linear mechanisms the rates can be obtained directly from the transfer function.

For a linear system, superposition assures independent response to each frequency component of the input. The phase shift and amplitude of the product signal at the fundamental modulation frequency may be determined with a lock-in amplifier. One such measurement at an appropriate frequency is sufficient for a reaction dominated by single first order step. With multichannel systems the complete product waveform is available. We can obtain the response simultaneously for all the frequency components present in the input modulation.

We show the experimental determination of the transfer function schematically in Fig. 3. For a linear system the observed product time-of-arrival waveform is the convolution of the reactant beam modulation and the surface product formation kinetics, with contributions from the flight time distributions of the modulated reactant and product, and detector response.

### 2. Deconvolution

We use a program which deconvolves each of these factors by complex division in frequency space. First the detailed chopper function is constructed. As the opening in the rotating chopper wheel crosses the circular collimator aperture a trapezoidal wave is produced, although the deviation from a square wave is negligible for these experiments. The velocity distribution of the incident molecular beam is reconstructed from fit parameters. The beam time of flight was measured independently, and fit to a shifted Maxwellian distribution

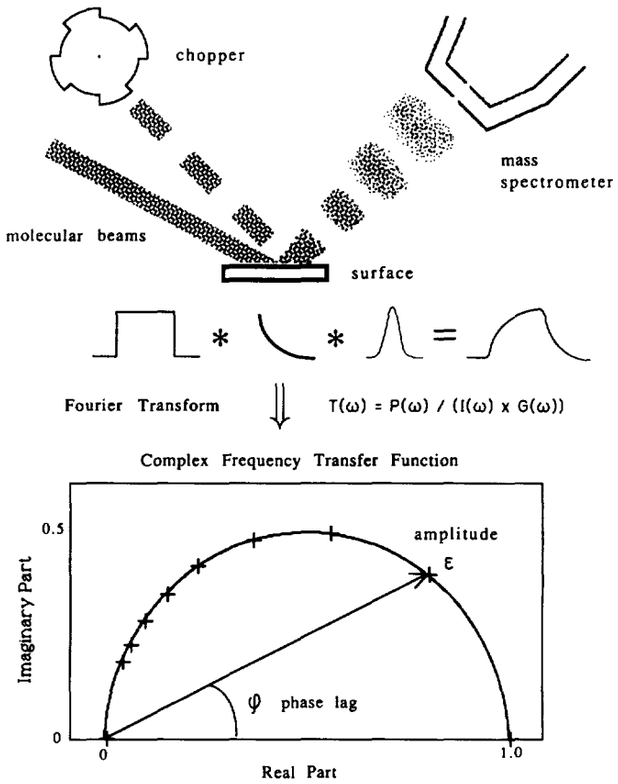


FIG. 3. A schematic of the transfer function analysis of MBRS for a linear system. The product flux is the convolution of the modulation, surface response, and instrumental and velocity functions. We wish to extract the surface response.

$dN/dv = Cv^3 \exp[-(v - v_0)^2/\alpha]$ with stream velocity $v_0$ and velocity spread $\alpha^{1/2}$. The distribution of the product flux is assumed to obey a Maxwell–Boltzmann form $dN/dv = Cv^2 \exp(-v^2 m/2kT)$, usually at the surface temperature. There is also a small time spread in the ionizer which varies with mass.

The product time-of-arrival waveform is Fourier transformed and normalized. It is then divided by the transformed chopper, beam velocity, product velocity, and ionizer functions. The result is the frequency domain transfer function. Taking frequency as a parameter we can use a compact complex representation. This is a polar plot of amplitude vs. phase for each frequency. Our calculations are usually in the equivalent, if less intuitive, Cartesian form as the imaginary and real parts of the complex transfer function.

### 3. Transfer functions for prototypic linear mechanisms

A number of excellent reviews of modulated beam reactive scattering have included transfer function analysis.[5,8] Due to its central role in this work, we will again outline some standard results.

A linear reaction network may consist of any series or parallel arrangement of linear steps. Several simple linear

reaction networks present characteristic transfer functions. We demonstrate the analysis for the simplest case of atomic adsorption–desorption

$$N_{gas} \underset{k}{\overset{s}{\rightleftarrows}} N_{ads}. \tag{12}$$

The rate equation is derived as usual from mass balance

$$\frac{dn_{ads}}{dt} = sn_{gas}(t) - kn_{ads}(t), \tag{13}$$

$n_{gas}$ is the reactant flux, $n_{ads}$ the surface density. Now the complex Fourier transform gives the frequency domain representation

$$-i\omega N_{ads}(\omega) = sN_{gas}(\omega) - kN_{ads}(\omega). \tag{14}$$

The differential equation has been transformed to an algebraic equation, which can be solved directly

$$N_{ads}(\omega) = \frac{sN_{gas}(\omega)}{k - i\omega} = \frac{sN_{gas}(\omega)(k + i\omega)}{k^2 + \omega^2}. \tag{15}$$

The frequency domain transfer function is the output divided by the input:

$$H(\omega) = \frac{kN_{ads}(\omega)}{N_{gas}(\omega)} = \frac{s[1 + i(\omega/k)]}{1 + (\omega/k)^2}. \tag{16}$$

In polar form, this expression gives the amplitude and phase lag of the response at each frequency

$$H(\omega) = s[1 + (\omega/k)^2]^{-1/2} e^{i\phi}, \quad \tan\phi = \omega/k. \tag{17}$$

To compare transfer functions, we will scale them by their steady state or zero frequency component, in this case $H(0) = s$. The impulse response to this single step process is a simple exponential decay, and the transfer function is a semicircular arc, as was shown in Fig. 3. Transfer functions for more complex linear mechanisms may be derived similarly. A few are shown in Fig. 4, others may be found in the references cited above.

### 4. $CO_2$ and $H_2O$ transfer functions

In Fig. 5 we compare transfer functions for carbon monoxide oxidation, $CO + O_2 \rightarrow CO_2$, and for hydrogen oxidation, $H_2 + O_2 \rightarrow H_2O$, both on the Rh(111) surface, over a similar temperature range. The $CO_2$ reaction is effectively first order in CO, perhaps because an excess flux of $O_2$ maintains a saturation coverage of atomic oxygen. For hydrogen oxidation this simplification is not possible; excess oxygen throttles the reaction. The transfer function for $CO_2$ is the characteristic single step arc. Changes in surface temperature or beam modulation frequency simply rotate the points along the arc. $H_2O$ is not a single step, but shows the pattern of a serial mechanism. The transfer function shifts with temperature as the relative rates of the serial steps vary.

Lock-in detection gives the phase and amplitude at the fundamental modulation frequency. The full time-of-arrival wave form acquired with a multichannel scaler system may be Fourier analyzed to give the response at each component

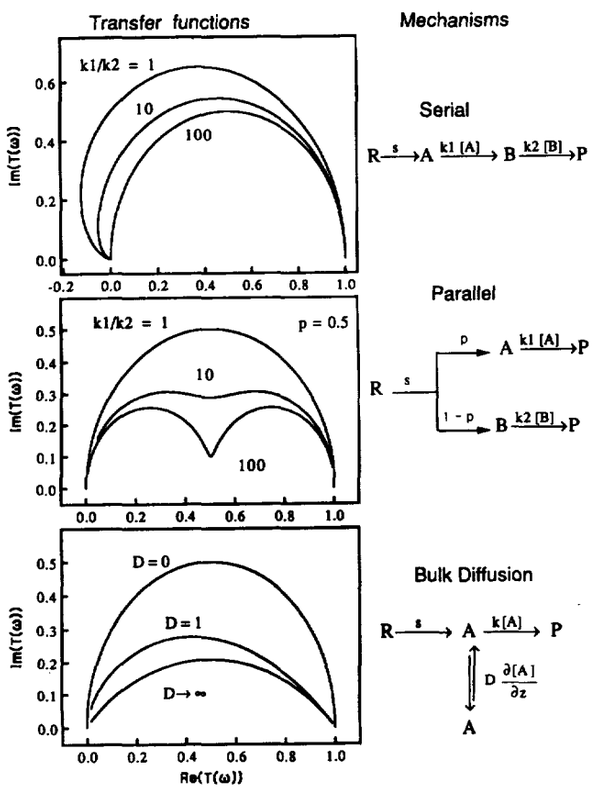


FIG. 4. Characteristic transfer functions for several simple linear reaction networks.

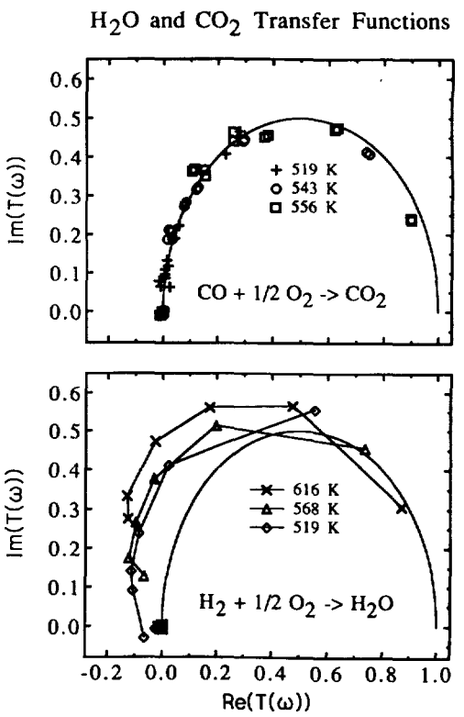


FIG. 5. Transfer Functions for $CO_2$ and $H_2O$. Carbon monoxide oxidation on Rh(111) is pseudo-first order, and the transfer function is a semicircle. Under similar conditions, $H_2O$ formation is not a single first order step, but appears as a series mechanism. The rate ratios vary with temperature.

frequency of the input. Superposition insures that the response at each frequency is independent, so the two techniques are equivalent for linear systems, though several measurements at different frequencies would be required with a lock-in. Note however, that the first harmonic in both reactions is close to the arc, so that lock-in measurements at only one frequency would not reveal the deviation from a single step.

## D. Nonlinearity

The preceding analysis, based on Fourier transform techniques, can only be applied to linear systems. The mechanisms for hydrogen recombination and water production outlined above in Eqs. (1)–(11) each contain several nonlinear factors. Whether nonlinearity is apparent in a particular experiment depends on the conditions and actual values of the rate constants. For water production above the peak temperature of 600 K we find linear responses over the accessible range of reactant pressures. This is an important clue in relating measured rates to steps in the postulated mechanism. For instance, it is immediately clear that hydroxyl disproportionation cannot be a major pathway at high temperatures. At lower temperatures however, the reaction does become strongly nonlinear, as we will show in a moment.

For a linear network we may expect the transfer function to vary with temperature as the relative rates shift. For fixed temperature however, the response should be a unique function of frequency. The transfer function plot is the locus of points for all frequencies, though any experiment gives only a finite set. As we change the fundamental period of the modulation, we expect the points to fall on a common curve for all frequencies present, regardless of the frequency spectrum of the modulation. If the set of points for different fundamental frequencies appear to delineate separate curves, we suspect that the response at each component frequency is affected by the other components. This interaction indicates that superposition does not hold, and that the system is not linear. This is the case for $H_2O$ at low temperatures, as seen in Fig. 6.

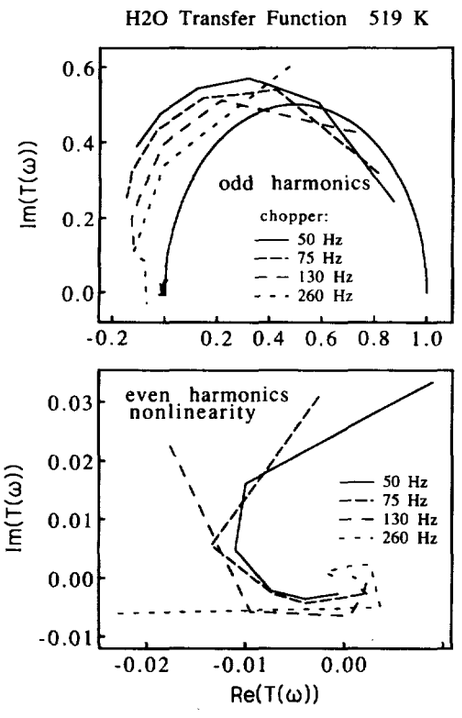


FIG. 6. $H_2O$ Nonlinearity. At low temperatures the $H_2O$ transfer function varies with modulation frequency. This is evidence of a nonlinear response. More definitive is the presence of even harmonics in the output which are not present in the square wave modulated input.

A clearer violation of superposition is the appearance of even harmonics in the product wave form. The chopper wheel produces a square wave reactant modulation, which is composed solely of odd harmonics of the fundamental. The presence of even harmonics in the product wave form above experimental noise indicates nonlinear kinetics. We see this at the bottom of Fig. 6.

Beside prohibiting deconvolution, nonlinearity presents severe mathematical difficulties in analyzing mechanisms. To understand a reaction, we usually wish to compare experimental results to a proposed model to establish the mechanism and relate the measured rate constants to the elementary steps. A model mechanism yields a set of ordinary differential equations describing the rates. For nonlinear differential equations there are no general mathematical techniques providing analytical solutions. We can sometimes study the model by numerical integration of the differential equations, but integration of chemical reaction mechanisms can be difficult. Rate constants for elementary reaction steps may range over many orders of magnitude, which creates numerical instabilities, or "stiffness."[16] Numerical solutions may also not yield the insight into the global behavior of the reaction that can come from analytic solutions.

## E. Multiple source MBRS

Now consider the general problem of modulated beam experiments on nonlinear reactions, schematized in Fig. 7. For a small modulated beam flux the response may be linear, but is restricted to a low coverage regime. Depending on the order, there may be little signal at all. If an intense modulated beam is used, we span a wide coverage range, but the highly nonlinear response is difficult to analyze.

A general approach to molecular beam studies of nonlinear surface kinetics has been known in principle for many years: the use of a small modulation superimposed on a continuous reactant flux. This is represented in Fig. 8 adapted from Ref. 3. For a sufficiently small perturbation, relaxation to the steady state is linear. If this linearization can be performed for different steady state conditions, the reaction mechanism or coverage dependence of the rate constants may be studied over the global range of conditions for the nonlinear reaction.

It is this scheme which we have implemented in the most direct manner—an additional molecular beam source. The arrangement for the present set of experiments was depicted in Fig. 1. Continuous beams of oxygen and hydrogen pro-

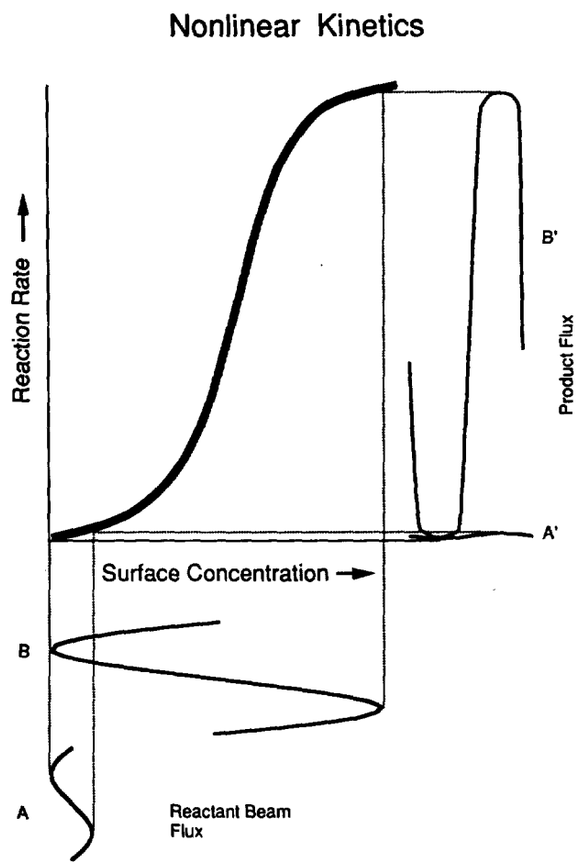


FIG. 7. This and the following figure, modeled after Ref. 3, depict a system for which the reaction rate is a highly nonlinear function of coverage. In such cases, conventional modulated beam experiments may fail. For small modulated beams we obtain a linear response, but we are restricted to low surface coverage, and there may be little signal. Intense modulated beams probe a wide coverage range, but the nonlinear response is difficult to analyze.

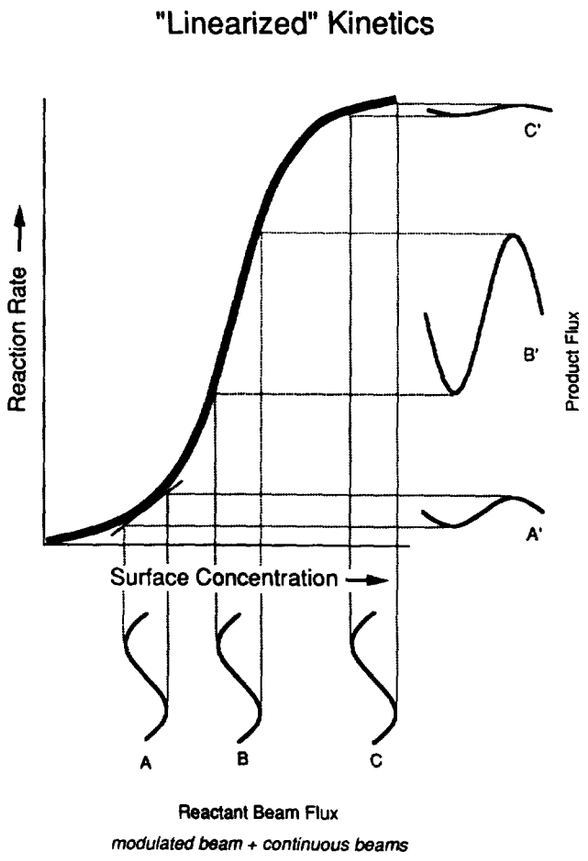


FIG. 8. A solution is to establish a steady state, then weakly perturb it so that relaxation is linear. By superimposing a small modulation on an adjustable continuous flux we obtain linear responses over a wide range of controlled coverages.

duce steady state surface coverages of reactants and intermediates; atomic oxygen and hydrogen, and hydroxyl. A weak modulated beam of hydrogen produces a perturbation of the steady state. When this perturbation is sufficiently small, water production will be linear. The continuous beam fluxes may be adjusted to vary the steady state coverages, and the reaction thus analyzed by linear techniques over a range of conditions. Isotopic substitution in the beams will be used to illustrate this linearization and to attempt to isolate individual reaction steps.

Use of a background pressure of reactant for linearization is not satisfactory, as the central advantages of molecular beams; high surface fluxes with low backgrounds, are lost. Two molecular beams are adequate for the HD reaction. Two beams may also suffice with two reactant species if reaction can only occur on the surface under study. In this case, a mixed continuous beam might be used with the modulated beam. The general utility of three beams is clear in hydrogen oxidation, where reactant mixtures are undesirable.

### *1. Controlling surface reactant coverages.*

At low temperatures, the water reaction was nonlinear, as shown in Fig. 6 for 520 K. At even lower temperatures the signal became erratic, depending on the history of beam fluxes and surface temperature. We suspect that at low temperatures the oxygen coverage would grow in between chopper pulses, and that reaction stopped if the surface was allowed to saturate with oxygen.

Using a continuous hydrogen beam in addition to the continuous oxygen and modulated hydrogen beams, we can to some extent control the hydrogen to oxygen ratio on the surface. The continuous hydrogen flux may prevent oxygen saturation between chopper pulses of modulated hydrogen. We can thus greatly increase the signal for low surface temperatures, as shown in Fig. 9 at 465 K. That this is possible again demonstrates that the response to hydrogen flux is not additive. If it were linear, the modulated product response would be independent of continuous hydrogen flux. The lower figure shows waveforms at 495 K, with and without a continuous hydrogen flux. The waveform with the continuous beam is slower. Not only is the total reaction yield nonlinear, but the kinetics vary as well!

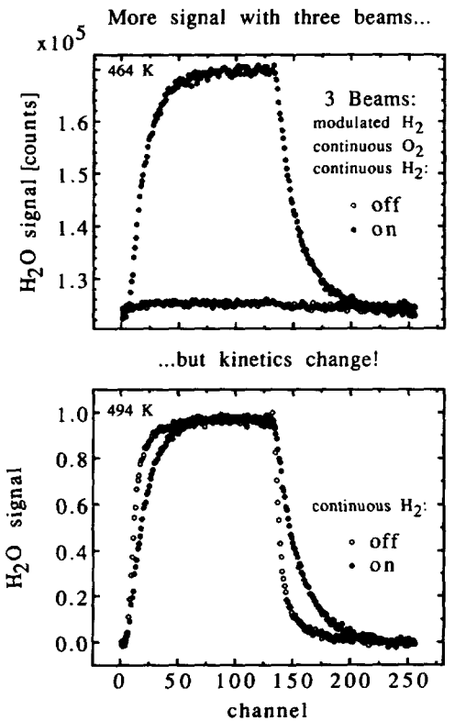


FIG. 9. Coverage dependent kinetics. The use of three beams; modulated hydrogen, continuous oxygen, and continuous hydrogen, not only results in greatly increased signal levels, but also reveals coverage dependent kinetics.

## 2. Coverage dependent rate constants

Figure 10 shows the effect of a continuous hydrogen beam on surface oxygen coverage, modulated water, and background. We focus on oxygen coverage as it can be easily determined by Auger spectroscopy. More importantly, the two continuous beams control the hydrogen to oxygen ratio and the amount of hydroxyl intermediate on the surface, which we could not directly measure. We now consider an experiment which attempts maximal control over reaction conditions. The two continuous beams are used to vary the steady state surface coverages, while the response to the modulated beam is recorded as a function of temperature, and multiple rates extracted by transfer function analysis.

First the crystal was placed in Auger position, inclined 45° to the incident beams. The flux in the continuous beam of $H_2$ was set and the steady state oxygen coverage measured. Rotating the crystal 90° placed it normal to the mass spectrometer, again at 45° to the beams. Waveforms were taken at several temperatures over the narrow range 640–690 K. At the end of the temperature scan, the crystal was returned to Auger position and the oxygen coverage measured. The continuous beam flux was then changed, and the procedure repeated for the new steady state. Note that the Auger and mass spectrometer positions were symmetric with respect to the incident beams, so that the beam fluxes and oxygen coverage on the surface were identical.

Transfer function analysis of the waveforms showed an essentially linear, serial reaction for this regime. The transfer functions were then fit to a two step serial process, yielding two rates for each run. Fig. 11 is an Arrhenius plot for these two rates at each steady state beam flux and temperature. The slopes of each set are roughly constant, giving activation energies of 10 and 2.5 kcal/mol, independent of oxygen coverage. The intercepts or pre-exponentials, however, show a general increase with oxygen coverage.

Suppose we had a step with oxygen as a reactant, but that the oxygen coverage was held constant while we modulated hydrogen. We would measure a pseudo-first-order rate with the constant oxygen coverage as a factor in the preexponential. The preexponential would approach zero as oxygen coverage decreased. This was not the case. Oxygen must have a more indirect influence.

Despite care that steady state had been reached, the oxygen coverage sometimes varied substantially during a run. This instability prevented a detailed determination of the coverage dependent rates. Nonetheless, this experiment does

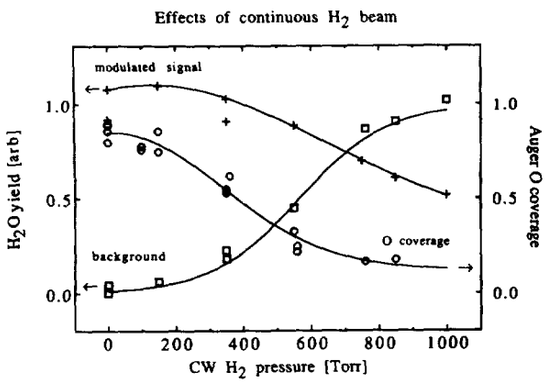


FIG. 10. Coverage control. The modulated $H_2O$ signal, background, and Auger oxygen peak as a function of the continuous hydrogen flux. The continuous hydrogen beam may be used to control coverages of oxygen and presumably hydroxyl.

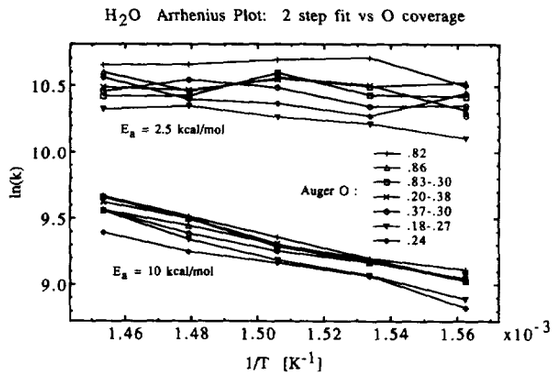


FIG. 11. Serial Arrhenius plot at different oxygen coverages. Two series rates extracted from the transfer function. This figure shows the two rates as a function of both temperature and oxygen coverage. The activation energies are relatively constant, but the preexponentials vary in a systematic fashion.

illustrate the potential of the multiple beam approach—we varied the steady state conditions with the two continuous beams, and used the perturbation induced by the modulated beam to examine the kinetics. Analysis of the full waveform then allowed us to extract several rates simultaneously.

### F. Isotopes and nonlinearity

We next show some remarkable results for water formation using isotopic substitution in three beams. We will then take a detour through hydrogen recombination to uncover the origins of a particular nonlinearity and give an example of the perturbation analysis of a linearized mechanism. We then return to water to demonstrate the linearization of the reaction. More results on water formation and analysis of the mechanism will appear in a separate publication.[9]

#### 1. $H_2+D_2+O_2$

When a continuous beam of $D_2$ is used along with a continuous beam of $O_2$ and modulated $H_2$, three isotopic forms of water are produced. Our idea was to isolate the H + OD step using large continuous fluxes of oxygen and deuterium to saturate the surface with OD. We would then examine the HDO produced by a small modulated hydrogen beam. Initially, we used a large modulated $H_2$ flux, and obtained waveforms for the three products shown in Fig. 12. The $H_2O$ wave form has the usual symmetric form. The HDO product however, shows a highly asymmetric waveform; a rapid rise, sloping top, and long decay. The $D_2O$ wave is very interesting. Since neither the $O_2$ nor $D_2$ beams were modulated this should produce a continuous background $D_2O$ flux. The negative modulation must be induced indirectly by the chopped $H_2$ beam. The modulated flux is perturbing the steady state surface coverages, and the depression of $D_2O$ production is a direct measure of this perturbation.

We have simulated this reaction by numerical integration of a rather elaborate model. The mechanism is essentially that of Eqs. (1)–(11) with the additional steps involving deuterium. Rates constants are estimated from several sources.[14,15,17] The results, shown in Fig. 13, show similar qualitative features to the observed waveforms. Unfortunately, this model contains too many parameters to clarify the mechanism

#### 2. $H_2+D_2$

The details of the model turn out to be irrelevant. The essential features of the isotopic water waveforms can be understood in the much simpler hydrogen–deuterium recombination reaction $H_2 + D_2 \rightarrow 2HD$. Here we see the same asymmetric waveform as in HDO, Fig. 14. The HD transfer function does not fall on the first order arc and has significant even harmonics.

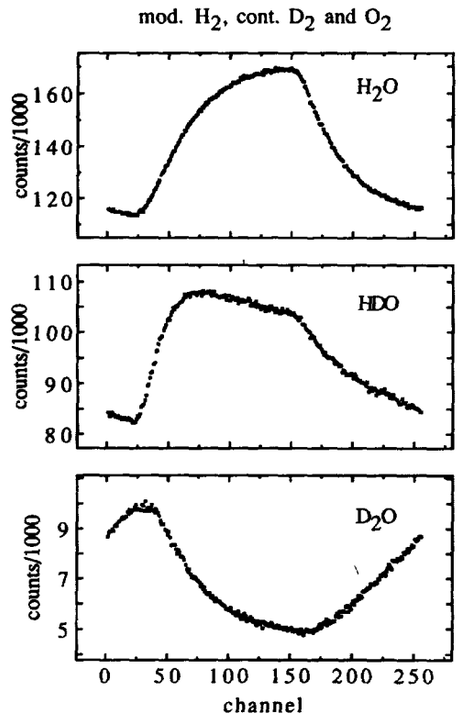


FIG. 12. Isotope experiment. The three isotopic water waveforms produced with modulated hydrogen, continuous oxygen, and continuous deuterium beams. The $H_2O$ wave form is as usual, the HDO waveform asymmetric, and the $D_2O$ waveform inverted! Note that both deuterium and oxygen are not modulated, and so the modulation of $D_2O$ is an indirect effect due to the perturbation of surface O or D by the modulated hydrogen flux.

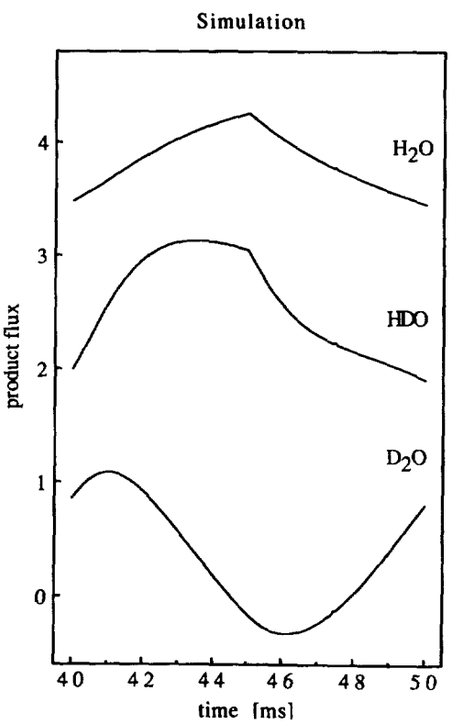


FIG. 13. Simulation. A model mechanism was numerically integrated to simulate the isotope experiment. The simulation was for a lower temperature than the experiment for ease of computation. The results are qualitatively similar.

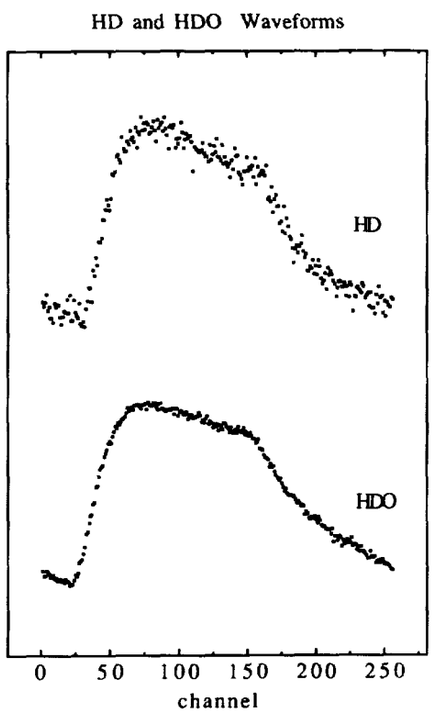


FIG. 14. The essential features of the asymmetric HDO waveform are also seen in an HD waveform.

Using the mechanism

$$H_{2gas} \underset{k_d}{\overset{s_0[1-([H]+[D])]}{\rightleftarrows}} 2H, \tag{18}$$

$$D_{2gas} \underset{k_d}{\overset{s_0[1-([H]+[D])]}{\rightleftarrows}} 2D, \tag{19}$$

$$H + D \xrightarrow{k_d} HD_{gas}. \tag{20}$$

We have simulated this reaction by numerical integration of the system

$$\frac{d[H]}{dt} = 2P_{H_2}\{1-([H]+[D])\} - 2k_d[H]^2 - k_d[H][D], \tag{21}$$

$$\frac{d[D]}{dt} = 2P_{D_2}\{1-([H]+[D])\} - 2k_d[D]^2 - k_d[H][D], \tag{22}$$

$$\frac{d[HD]_{gas}}{dt} = k_d[H][D]. \tag{23}$$

Results are shown in Fig. 15. The qualitative behavior does not depend on the rate constants, only on the ratio of the modulated to continuous fluxes. We see the asymmetric wave form at top left-hand side. The transfer function for the simulation is shown at bottom, it falls inside the single step arc and is nonlinear. The surface coverages are at top right. As the modulated H coverage increases, the steady state D coverage drops. The rapid rise is due to the increase in H, the sagging top to decline in D. The long tail is from the recovery of D as H decreases; the product of the two drops less quickly than H alone.

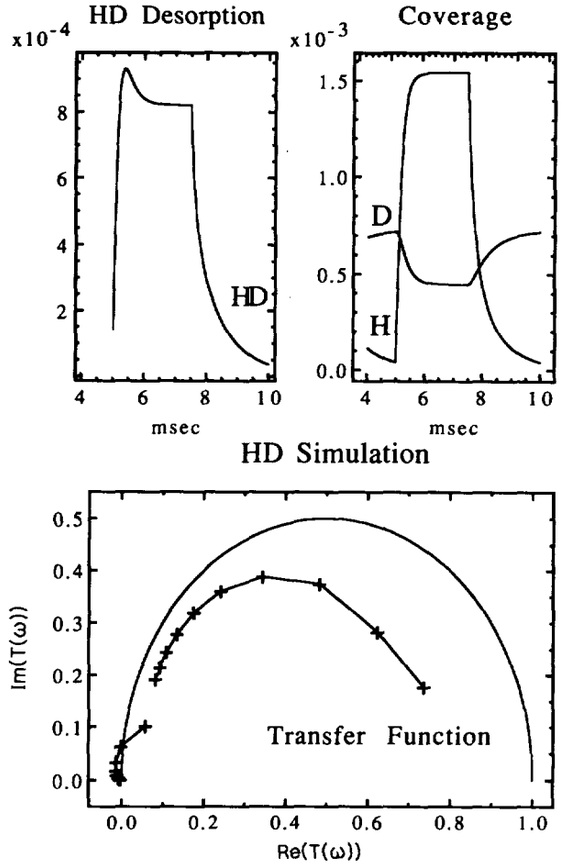


FIG. 15. A simulation of $H_2 + D_2$ recombination. The waveform is top left, surface coverages top right, and the transfer function bottom. The large modulated hydrogen beam flux perturbs the steady state surface coverage of deuterium. Since the HD flux is the product of the two coverages, the HD wave is asymmetric and nonlinear. The surface temperature was 650 K, beam fluxes 1–5 ML/s, $s_0 = 0.65$, $k_d{:}E_a = 20$ kcal/mol, $A = 10^{-3}$ cm$^2$ s$^{-1}$.

This is the crux of the problem: the asymmetry, and nonlinearity, arises from perturbation of the steady state surface coverage by the modulated reactant. Reducing the intensity of the modulated beam reduces the nonlinearity. In Fig. 16 simulation matches the qualitative features of the experiment. As the modulation is decreased, the wave form becomes more symmetric, the transfer function approaches the single step arc, and the even harmonics vanish. In the limit of a small perturbation, this reaction becomes linear.

## G. Perturbation analysis for $H_2$

In this small perturbation limit it is possible to analytically solve the differential equations for the mechanism. We illustrate this for the simplest case of hydrogen recombination. The reaction is second order in hydrogen concentration, and thus nonlinear.

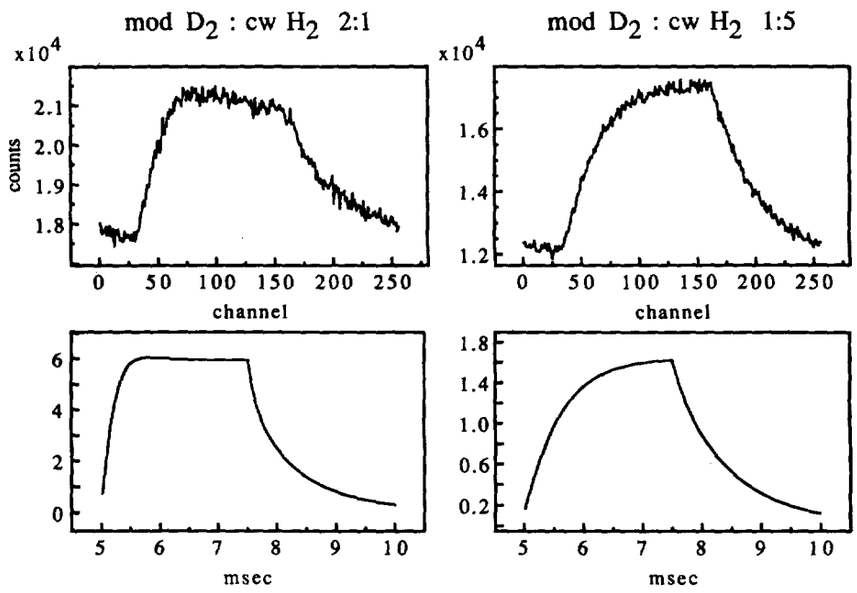


FIG. 16. Simulated and experimental HD wave forms show similar behavior as the modulation ratio changes.

$$H_{2gas} \underset{k}{\overset{s}{\rightleftarrows}} 2H. \tag{24}$$

The sticking coefficient is $s$, the desorption rate $k$. Let the reactant flux be $P$ and the surface concentration of hydrogen [H] then

$$\frac{d[H]}{dt} = 2sP - 2k[H]^2. \tag{25}$$

Now consider a small time dependent flux superimposed on a continuous background $P = p_0 + \epsilon p(t)$. We wish to obtain a solution in the form $[H] = h_0 + \epsilon h(t)$. We then have

$$\frac{d[h_0 + \epsilon h(t)]}{dt} = 2s[p_0 + \epsilon p(t)] - 2k[h_0 + \epsilon h(t)]^2 \tag{26}$$

or

$$\frac{d(h_0)}{dt} + \epsilon\frac{dh(t)}{dt} = 2sp_0 + \epsilon 2sp(t) - 2kh_0^2 - 4k\epsilon h_0 h(t) + 2k\epsilon^2 h(t)^2. \tag{27}$$

If this is to hold for all values of $\epsilon$ over some interval, then the coefficients of each power of $\epsilon$ must equate. For zeroth order we have the steady state component

$$\frac{dh_0}{dt} = 0 = 2sp_0 - 2kh_0^2. \tag{28}$$

This yields $h_0 = \sqrt{sp_0/k}$, the steady state surface coverage. The first order perturbation is

$$\frac{dh(t)}{dt} = 2sp(t) - 4kh_0 h(t). \tag{29}$$

This is the desired linear response. Substituting the steady state $h_0$,

$$\frac{dh(t)}{dt} = 2sp(t) - 4kh(t)\sqrt{sp_0/k} \tag{30}$$

or

$$\frac{dh(t)}{dt} = 2sp(t) - 2k'h(t), \tag{31}$$

where the effective rate constant $k' = 2\sqrt{skp_0}$. In Arrhenius form we have

$$A' \exp(-E'/kT) = 2\sqrt{sp_0 A}\exp(-E/kT), \tag{32}$$

with $A' = 2\sqrt{sp_0 A}$ and $E' = E/2$. Finally we relate the measured rates for the linearized system to the actual rates

$$A = \frac{A'^2}{4sp_0}, \quad E = 2E'. \tag{33}$$

Note that it is necessary to analyze the linearized mechanism to determine the relationship between the actual constants for the elementary steps and the pseudo-first order rates that are measured. In this case the activation energy is obtained immediately, while the preexponential requires knowledge of the beam flux and sticking coefficient, or of the steady state coverage $h_0$. An Arrhenius plot for the apparent rates is shown in Fig. 17. The pseudo-first order rate constants were $E_a' = 10.0$ kcal/mol, $A' = 10^7\,s^{-1}$. The true second order constants were $E_a = 20$ kcal/mol, $A = 10^{-2}$ $cm^{-2}\,s^{-1}$. This is in good agreement with earlier work.[15,18]

## H. HDO linearization

We now return to the isotopically substituted water reaction. As for HD, we wished to reduce the modulation until the HDO response is linear. Fig. 18 shows the evolution of the HDO transfer function as the intensity of the modulated H beam was reduced. The odd harmonics move toward the

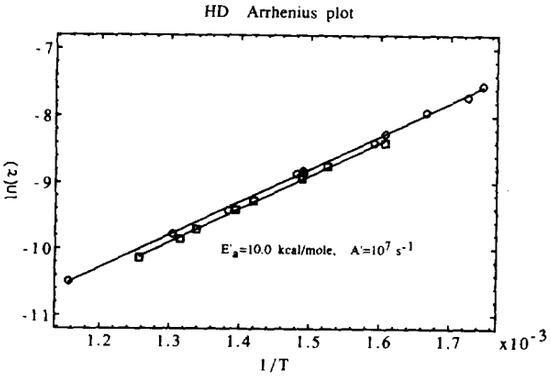


FIG. 17. HD Arrhenius plot. Linearized or pseudo-first order rates for $H_2$–$D_2$ recombination are plotted. The true second order rates are derived from them: $E_a = 2E'_a$ or 20 kcal/mol, the preexponential is $\approx 10^{-2}$ $cm^2\ s^{-1}$, using an estimated continuous beam flux of 10 ML/s which varied slightly between runs.

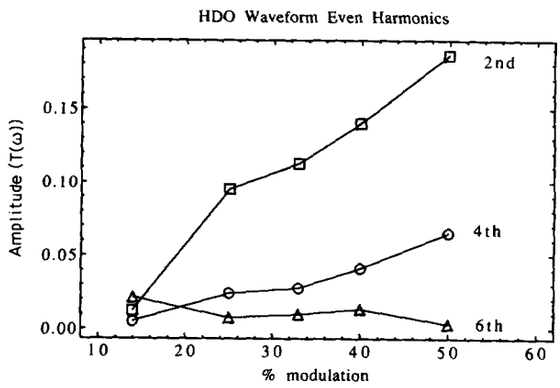


FIG. 19. HDO linearization. Derived from the previous plot, we show the modulus of the even harmonics vs modulation. This clearly demonstrates the linearization of the kinetics in the limit of small modulation.

single step arc, and the amplitude of the even harmonics decrease. In Fig. 19, the amplitude of the even harmonics is plotted against the modulation. Modulation is given as the ratio of the modulated $H_2$ beam flux to the sum of $H_2$ and $D_2$ fluxes. This clearly shows the linearization of the response in the limit of small modulation. In this limit, the modulation does not perturb the steady state coverages of reactants and intermediates. The continuous oxygen and deuterium beams allow us to measure the perturbation of the surface coverages. The depression of steady state $D_2O$ evolution indicates that the smallest modulation produced a perturbation of only 0.6%.

It is easy to obtain waveforms in the nonlinear regime, but to obtain good data which is completely linear is a challenge. The bottom of Fig. 20 is a waveform with 40% perturbation

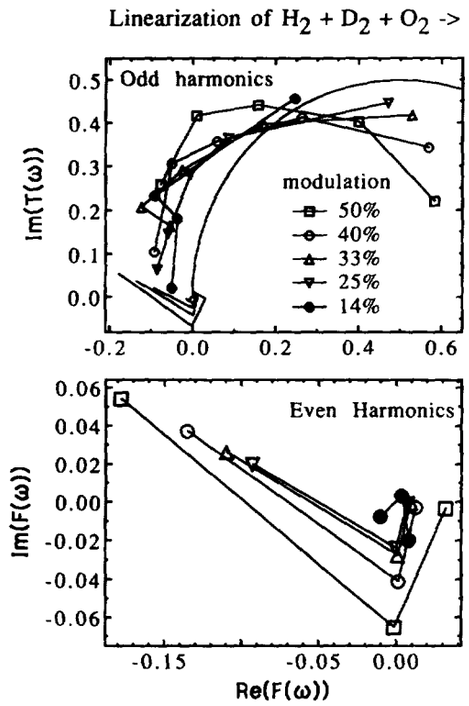


FIG. 18. The HDO transfer function is shown with varying modulation levels. Modulation is $P_H(\text{mod})/[P_H(\text{mod}) + P_D(\text{cont})]$. The sequence of first harmonic points (upper plot, right side) moves toward the single step semicircle. The second harmonics (bottom plot, left side) move toward (0,0) for decreasing modulation.

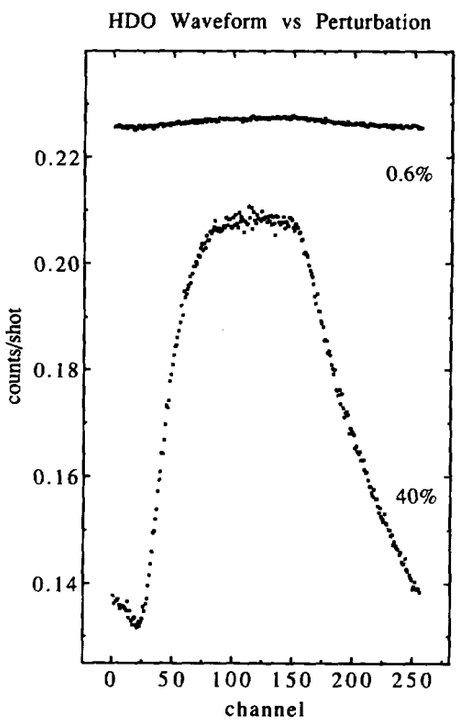


FIG. 20. Signal vs perturbation. The bottom waveform used a modulated $H_2$ beam which perturbed the continuous $D_2O$ background by 40%. In the top waveform the modulated beam perturbed the steady state by less than 1%.

acquired in 20 min. The top is a waveform for a perturbation of 0.6%, the most linear point in the previous figure. This waveform required 8 hours of data collection and represents 10 million chopper pulses. Subsequent experiments were less ambitious, but as a consequence the data still show slight nonlinearities. The full perturbation analysis for the mechanism of Eqns. (1)–(11) is essentially similar to that for HD, but the relationship of the effective rates to the elementary steps is much more complicated. Further results may be found in Ref. 9.

## IV. CONCLUSION

We have introduced a novel *three* molecular beam arrangement which increases the power and versatility of linearized MBRS. Using two continuous, independently variable reactant beams we can choose and control steady state surface coverages, while a modulated beam probes the kinetics by perturbing this steady state. Sufficiently small perturbations of the steady state allow the linearization of nonlinear kinetics. The ability to control surface coverages is necessary to study coverage dependent rate constants. Exploring a wide range of coverages, perhaps with different isotopes in the beams, may uncover regimes where different reactions dominate the kinetics. This can help to isolate single elementary steps and unravel complex reaction networks.

As examples, we examined hydrogen–deuterium recombination and the oxidation of hydrogen to water on the Rh(111) surface. HD gave a simple example of experimental linearization and the associated perturbation expansion analysis of the mechanism. The more complex water reaction illustrated the ability to study a reaction over an extremely wide range of conditions. We saw linear and nonlinear reaction regimes, and varied oxygen coverages to control the reaction and examine the coverage dependence of rate constants. Using modulated hydrogen with continuous oxygen and deuterium beams to produce the three water isotopes gave unusual waveforms which provide a striking example of nonlinearity and its elimination.

The technique presented here allows us to explore nonlinear surface reaction kinetics using a very general combination of experimental and analytical strategies. Both HD and HDO reactions were moved from nonlinear to linear regimes experimentally by reducing the intensity of the modulated flux relative to continuous reactant flux. Fourier transform deconvolution and other linear analysis methods could then be applied to the data. The sets of coupled differential equations describing postulated mechanisms were then solved by perturbation expansion in the concentration variables. Thus the experimental and mathematical approaches, each based on linearity in the limit of small perturbations around a selected steady state, possess an appealing symmetry.

## V. FURTHER DEVELOPMENTS

The method we have described is simple and direct, offers great flexibility in experimental design, and leads naturally to a perturbation analysis of proposed mechanisms. However, the relation between the measured rates and the elementary steps of a mechanism may be complicated. It is often necessary to have an independent means of measuring surface coverages. Other instrumentation can be effectively combined with modulated beams, such as Auger, electron energy-loss spectroscopy or Fourier transform infrared. We are investigating the concurrent use of helium reflectivity to measure surface coverage.[12,19] We would also like to mention related techniques for nonlinear surface kinetics. Besides the frequency domain methods we have outlined there are also direct time domain analyses of modulated beam kinetics.[20] Another promising method, which does not require modulated beams, is surface temperature modulation. This should be useful in determining activation energies for many nonlinear reactions.[21]

## ACKNOWLEDGMENTS

This work was supported in part by the Office of Naval Research, and by the NSF Materials Research Laboratory program at the University of Chicago (NSF-DMR-8819860).

a) Current address: Department of Chemistry, University of California, Berkeley, CA 94720.

[1] M. Eigen in *Technique of Organic Chemistry* (Interscience, New York, 1963), Vol. VIII, Part II, p. 901.
[2] H.-C. Chang and W. H. Weinberg, J. Chem. Phys. **66**, 4176 (1977).
[3] C. T. Foxon, M. R. Boudry and B. A. Joyce, Surf. Sci. **44**, 69 (1974).
[4] D. R. Olander and A. Ullman, Int. J. Chem. Kinetics **8**, 625 (1976).
[5] J. A. Schwarz and R. J. Madix, Surf. Sci. **46**, 317 (1974).
[6] R. H. Jones, D. R. Olander, W. J. Siekhaus, and J. A. Schwarz, J. Vac. Sci. Technol. **9**, 1429 (1972).
[7] H. H. Sawin and R. P. Merrill, J. Vac. Sci. Technol. **19**, 40 (1981).
[8] M. P. D'Evelyn and R. J. Madix, Surf. Sci. Rept. **3**, 413 (1984).
[9] D. F. Padowitz and S. J. Sibener, Surf. Sci. (in press).
[10] L. S. Brown and S. J. Sibener, J. Chem. Phys. **89**, 1163 (1988).
[11] K. D. Gibson and S. J. Sibener, J. Chem. Phys. **88**, 791 (1988).
[12] G. Comsa and R. David, Surf. Sci. Rept. **5**, 145 (1985).
[13] P. R. Norton in *The Chemical Physics of Solid Surfaces and Heterogeneous Catalysis*, edited by D. A. King and D. P. Woodruff, (Elsevier, New York, 1982), Vol. 4.
[14] P. A. Thiel, J. T. Yates, Jr., and W. H. Weinberg, Surf. Sci. **82**, 22 (1979).
[15] J. T. Yates, Jr., P. A. Thiel and W. H. Weinberg, Surf. Sci. **84**, 427 (1979).
[16] R. C. Aiken, editor, *Stiff Computation* (Oxford, New York, 1985).
[17] D. S. Y. Hsu, M. A. Hoffbauer and M. C. Lin, Surf. Sci. **184**, 25 (1987).
[18] T. Engel and H. Kuipers, Surf. Sci. **90**, 162 (1979).
[19] K. Peterlinz, T. Curtiss and S. J. Sibener (to be published).
[20] A. B. Anton and D. C. Cadogan, Surf. Sci. Lett. **239**, L548, (1990).
[21] J. R. Engstrom and W. H. Weinberg, J. Chem. Phys. **87**, 4211 (1987).
[22] T. Engel and H. Kuipers, Surf. Sci. **90**, 181 (1979).